INFLUENCE OF MEASURED SCATTERING PARAMETERS ON THE CONVOLUTION SIMULATION OF NONLINEAR LOADED HIGH-SPEED MICROSTRIP INTERCONNECTS

C. M. F. Cárdenas and A. D. Jiménez[*]

Departamento de Electrónica, Universidad de Guadalajara, Av. Revolución No. 1500, Guadalajara, Jalisco 44430, México

Abstract—The simulation of nonlinear loaded high-speed microstrip interconnects by means of a convolution-based procedure is described when both, analytical and measured scattering parameters are used. Closed-form equations are employed to obtain the analytical scattering parameters. The influence of measured scattering parameters, when these are used instead the analytical ones, is investigated to know how the microstrip interconnect responses are affected. The convolution procedure is complemented by including the transmission line linear equation and the microwave circuit reflection theory.

1. INTRODUCTION

Many different procedures for a transient analysis of nonlinear loaded microstrip interconnects have evolved and matured throughout the recent years. Both, analytical and numerical techniques based on the prediction of the scattering S-parameters have been presented for such a task. The prediction of the S-parameters is however only an approximation thereby in some cases leads to coarse or poor results. To reveal this inconvenience, the importance of using a novel procedure combining the measured real S-parameters and the transmission line reflection theory is emphasized when convolution simulations of microstrip interconnects are performed.

Perhaps some of the first works where the convolution (initially not called by its name) was used to perform transient analyses of

nonlinear loaded electromagnetic circuitry were reported by Tesche and Liu in 1975 and 1976 [1, 2]. The convolution was applied to time-domain variables obtained from the Fourier transform of frequency-domain data. A decade later, Yang et al. and Gu et al. [3, 4] presented time-domain analyses for microstrip transmission line systems (single and coupled) by using the convolution theory. By the same time, Djordjevic et al. [5, 6] analyzed time-domain responses of multiconductor transmission lines by means also of convolution. Afterward, a plethora of researchers [7–22] presented different applications of the convolution concept to simulate linearly and nonlinearly terminated transmission lines and high-speed microstrip interconnects. A more complete representation for the microstrip interconnects, based on a time-domain RLCG-model instead of the classic frequency-domain S-parameter-model was introduced in [23]. One of the most cited references is that of [9]. In that work, a recursive convolution-based simulation is derived by making use of Padé approximations. The Padé technique suffers however of generation of unstable poles for known stable networks [24]. A book treating deeply the recursive convolution is that of [25]. More recently, Chiu and Chiang [26] presented a convolution approach for analyzing the long-time response of high-speed dispersive and lossy interconnects terminated with nonlinear loads. Although nowadays the state of the art in modeling interconnects tends to the generation of parametric macromodels [27–31] where direct use of the time-consuming convolution process is omitted, the transient-analysis convolution-based technique is still completely applicable. A common factor in the papers treating the macromodels is a previously generated data obtained through a broadband measurement or electromagnetic simulation.

The authors of the fast-real time convolution algorithm presented in [26] claim their closed-form formulas for acquiring the scattering parameters are accurate and wideband effective. The formulas they derived are correct, but the assumptions are not, since the formulas neither are broadband operational nor reproduce accurately the real microstrip behavior. In this paper, the simulation of a diode loaded high-speed microstrip interconnects by using a convolution algorithm is performed when both, analytical and measured scattering parameters are used. To demonstrate the relevance of the proposed procedure and the differences between the responses, the algorithm is enhanced by adding the microwave circuit reflection theory.

2. THE MEASUREMENTS AND THE CONNECTOR DE-EMBEDDING PROCEDURE

The measurements were performed on connectorized microstrips thereby the connectors must be de-embedded in order to do the comparison between the analytical and experimental scattering parameters. The de-embedding technique is a simple one based on the shifts of the microstrip reference planes generated by the lengths of the coaxial connectors (SMA or K). The symmetric perturbations (same kind of male or female connectors at the input and output ports) caused by these shifts correspond to rotations of the immittance matrix unit amplitude eigenvalues through arbitrary phase angles [32, 33]. The procedure to extract the connectors is as follows:

1. From the connector characteristics, the total connector attenuation α_t is given by the sum the conductor α_c an dielectric α_d losses as [34]

$$\alpha_t = \alpha_c + \alpha_d \tag{1}$$

where

$$\alpha_c = \frac{R_s}{4\pi Z_0} \left(\frac{1}{a} + \frac{1}{b} \right), \tag{2}$$

$$\alpha_d = \frac{k \tan \delta}{2}, \tag{3}$$

R_s is the high-frequency surface resistance, Z_0 is the characteristic impedance of the coaxial connector, a and b are respectively the external and internal radii of the coaxial connector inner and outer conductors, $k = \omega \sqrt{\mu \varepsilon}$ is the wavenumber, $\omega = 2\pi f$ is the radian frequency, μ and ε are respectively the connector dielectric permeability and permittivity, and $\tan \delta$ is the loss tangent.

2. From the total attenuation and the connector lengths, the forward shift is calculated by means of a matrix transformation in the following way [35–37]

$$\mathbf{S}' = \mathbf{D}^{-1}\mathbf{S}\mathbf{D}^{-1} \tag{4}$$

where

$$\mathbf{D} = \begin{bmatrix} \exp(-j\theta_1) & 0 \\ 0 & \exp(-j\theta_2) \end{bmatrix}, \tag{5}$$

$$\mathbf{S} = \begin{bmatrix} S_{11} & S_{12} \\ S_{21} & S_{22} \end{bmatrix} \tag{6}$$

is the scattering matrix of the connectorized microstrip line, and

$$\mathbf{S}' = \begin{bmatrix} \exp(-j2\theta_1) S_{11} & \exp[-j(\theta_1 + \theta_2)] S_{12} \\ \exp[-j(\theta_2 + \theta_1)] S_{21} & \exp(-j2\theta_2) S_{22} \end{bmatrix} \tag{7}$$

is the scattering matrix of the microstrip line when the connectors have been de-embedded or extracted. The perturbations are symmetric when the electric length $\theta = \beta l$ is the same in both, the input and output ports. The electric length is directly proportional to both the frequency f, included in the phase constant $\beta = {}^{2\pi f}\!/_{v_{pm}}$, and the physical length l. The microstrip phase velocity v_{pm} is corrected with the lengthening factor f_l to obtain the correct resonant frequency [38–40].

To provide substantiation to the importance of using the characterized interconnect S-parameters instead of the analytical ones, graphs of comparison between the measured and the analytically obtained scattering parameters [26] are presented in Figs. 1 and 2 for two different microstrip line interconnects. The measurements were carried out by using an Agilent® 8714ES automatic network analyzer and a Rohde & Schwarz R&S® ZVA series vector network analyzer. One microstrip line was built on a substrate with a permittivity of $\varepsilon_r = 10.5$ and a thickness of $H = 0.0635$ cm with SMA male and female connectors. The strip length is of $l = 3.7$ cm and the strip width is of $W = 0.1882$ cm which correspond to an impedance of approximately $25\,\Omega$. Another microstrip line was fabricated on a substrate with a permittivity of $\varepsilon_r = 3.0$ and a thickness of $H = 0.0254$ cm with Anritsu® K female connectors [41]. The strip length is of $l = 5.0$ cm and the strip width is of $W = 0.06$ cm which correspond to an impedance of approximately $50\,\Omega$. As can be seen from Fig. 1

(a) (b)
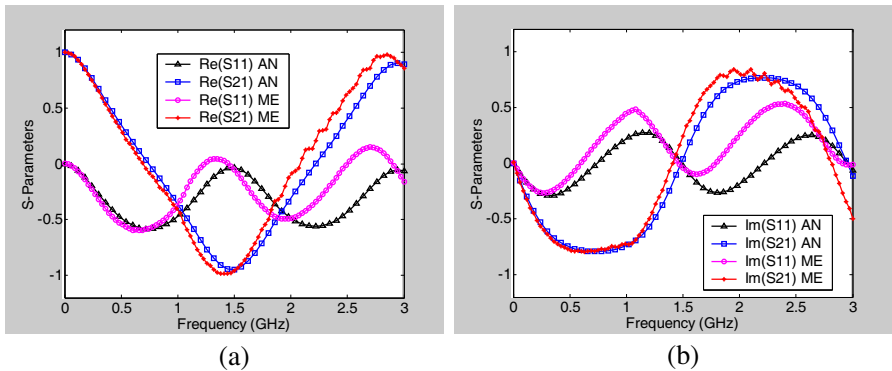
Figure 1. Measured (ME) and analytically (AN) obtained scattering parameters for a $25\,\Omega$ microstrip line interconnects built on a $\varepsilon_r = 10.5$ and $H = 0.0635$ cm substrate with a strip length of $l = 3.7$ cm and a strip width of $W = 0.1882$ cm. A female SMA connector is at the input port and a male SMA connector at the output port.
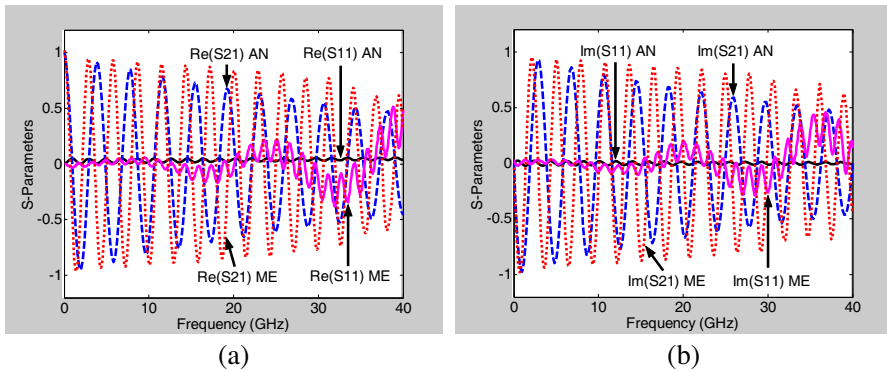
Figure 2. Measured (ME) and analytically (AN) obtained scattering parameters for a $50\,\Omega$ microstrip line interconnects built on a $\varepsilon_r = 3.0$ and $H = 0.0254\,\text{cm}$ substrate with a strip length of $l = 5.0\,\text{cm}$ and a strip width of $W = 0.06\,\text{cm}$. Female K connectors are at the input and output ports.

for the first microstrip line interconnects, a noticeable difference between the analytical (S_{11}, black; S_{21}, blue) and experimental (S_{11}, magenta; S_{21}, red) scattering parameters is easily appreciable in a bandwidth from 0 to 3 GHz. The real and imaginary parts of the analytical reflection and transmission parameters are more extended periodic curves (less cycles in the same bandwidth) compared to those of the measured reflection and transmission parameters. This mean the closed-form model may indeed represent electrically shorter or longer interconnects depending on the frequency and its physical length. As the bandwidth augments up to 40 GHz, the differences between the analytical (S_{11}, solid black; S_{21}, dashed blue) and measured (S_{11}, solid magenta; S_{21}, dotted red) scattering parameters augment significantly, not only in the number of cycles per bandwidth but also in the monotonic behaviour, mainly at the higher frequencies as can be seen in Fig. 2 for the second microstrip line interconnects. These differences will indubitably affect the convolution simulation results as will be seen in Section 4.

3. REFLECTION THEORY AND THE INTERCONNECT LINEAR EQUATION

From the microwave transmission line and reflection theories, a slight improvement to the response time of the convolution simulation algorithm, can be added by including the interconnect linear equation

and the input and output port reflections of a double terminated interconnect line. Thus, a system of equations to be solved is composed by the interconnect linear equation and the nonlinear equation at its port 2, which is given in terms of a convolution of time-domain functions ($*$) depending on the interconnect scattering parameters (S_{11}, S_{12}, S_{21}, S_{22}). The interconnect linear equation comes from the simultaneous solution of the transmission line load voltage and current equations given by [42]

$$V_L = V^+ + V^- \tag{8}$$

$$I_L = \frac{V^+}{Z_0} - \frac{V^-}{Z_0} \tag{9}$$

resulting

$$I_L = \frac{2V^+}{Z_0} - \frac{V_L}{Z_0} \tag{10}$$

where V^+ and V^- are unknown coefficients and represent waves traveling towards the load and towards the source respectively, Z_0 is the line characteristic impedance and V_L, I_L are the load voltage and current respectively. The nonlinear equation at port 2 is given by [26]

$$f\left(v_2\left(t\right)\right) = x\left(t\right) * v_2\left(t\right) + y\left(t\right) \tag{11}$$

where

$$x\left(t\right) = F^{-1}\left\{\frac{4Z_g S_{12}S_{21} - Z_g\Delta_1\Delta_2 - Z_r\Delta\Delta_2}{Z_r\Delta\left(Z_r\Delta + Z_g\Delta_1\right)}\right\}, \tag{12}$$

$$y\left(t\right) = F^{-1}\left\{\frac{2V_g S_{21}}{Z_r\Delta + Z_g\Delta_1}\right\}, \tag{13}$$

$$\Delta = \left(1 + S_{11}\right)\left(1 + S_{22}\right) - S_{12}S_{21}, \tag{14}$$

$$\Delta_1 = \left(1 - S_{11}\right)\left(1 + S_{22}\right) + S_{12}S_{21}, \tag{15}$$

$$\Delta_2 = \left(1 + S_{11}\right)\left(1 - S_{22}\right) + S_{12}S_{21}. \tag{16}$$

In (12) and (13), V_g denotes the Fourier transform of the voltage source $v_g\left(t\right)$; F^{-1} denotes the inverse Fourier transform and "$*$" stands for convolution. S_{11}, S_{12}, S_{21} and S_{22} are the S-parameters of the interconnect. Z_g and Z_r are the source impedance and the reference impedance at ports, respectively.

In (11), $v_2\left(t\right)$ denotes the voltage across the nonlinear load (a Shockley diode) and is declared as V_L in (10) and given by [43]

$$V_L = \ln\left(\frac{I_L}{I_S} + 1\right)nV_T \tag{17}$$

where I_S is the reverse bias saturation current, n is the ideality factor which in many cases is assumed to be approximately equal to 1 and V_T is the thermal voltage given by

$$V_T = \frac{kT}{q} \tag{18}$$

where k is the Boltzmann constant, T is the absolute temperature of the p-n junction and q is the magnitude of the elementary charge.

The procedure initiates by stating a first initial guess for V_L and I_L by simply taking values around the unity. Then, a first source voltage is settled down as the amplitude of a trapezoidal-pulse train which is implemented by using the trapezoidal membership function (TRAPMF) of Matlab$^®$. Next, a first V^+ value for (10) is obtained at time $t = 0$, from the voltage division of the source and line given by [38]

$$V^+ = V_g \left[\frac{Z_0}{(Z_g + Z_0)} \right]. \tag{19}$$

Subsequently, the reflection coefficient at the source is obtained as

$$\Gamma_g = \frac{Z_g - Z_0}{Z_g + Z_0}. \tag{20}$$

which will be used to attain the new V^+ value inside the system of equations-convolution loop. To solve this convolution dependant system, the Newtons and Jacob functions [44] as well as the FEVAL and CONV Matlab$^®$ functions are employed. With the value of V_L at hand, the first value of V^- is obtained from (8) as

$$V^- = V_L - V^+. \tag{21}$$

Accordingly, the convolution-based simulation is initiated by calculating the new V^+ value from the source voltage (the trapezoidal-pulse train or *pulse*) plus the reflected voltage from the source resistance ($\Gamma_g V^-$)

$$V^+ = pulse + \Gamma_g V^- \tag{22}$$

and starting the numerical solution of the linear-nonlinear system of equations followed by the assignation of new guess values from the recently calculated V_L and I_L, the calculation of the reflection coefficient at the load given by

$$\Gamma_L = \frac{Z_L - Z_0}{Z_L + Z_0}, \tag{23}$$

and the evaluation of the new V^- value from the reflected voltage coming from the load ($\Gamma_L V^+$) and given by

$$V^- = \Gamma_L V^+. \tag{24}$$

    This process is repeated until a determined number of time
iterations are reached. The iteration procedure is thus stated and
accomplished in a time marching fashion by updating the guess values
with the previously calculated V_L and I_L, each time iteration.

4. THE CONVOLUTION SIMULATION

By applying the above described procedure to the aforementioned
microstrip line interconnects the following results were obtained when
two different trapezoidal-pulse trains were used. Explicit applications
of the trapezoidal-pulse train to transmission line interconnects can be
found in [45, 46]. Considering the Fig. 5 of [26], the pulse train for the
$\varepsilon_r = 10.5$ interconnects was defined with an amplitude $A_p = 1\,\text{V}$, same
rise and fall times $\tau_r = \tau_f = 35\,\text{ps}$, $\tau = 1.5\,\text{ns}$ and $\tau_H = \tau_L = 0.715\,\text{ns}$;
the pulse train for the $\varepsilon_r = 3.0$ interconnects was defined with an
amplitude $A_p = 1\,\text{V}$, same rise and fall times $\tau_r = \tau_f = 210\,\text{ps}$,
$\tau = 9.0\,\text{ns}$ and $\tau_H = \tau_L = 4.29\,\text{ns}$. Fig. 3 shows the convolution
simulation responses for the $\varepsilon_r = 10.5$ microstrip line interconnects
when the scattering parameters obtained from the closed-form formulas
(blue) and those by using the measured scattering parameters (red) are
used. Fig. 4 shows in addition, the response of a three times electrically
longer microstrip line interconnects by using the scattering parameters
obtained from the closed-form formulas (green). As can be seen from
this figure the red and green curves differ substantially from the blue
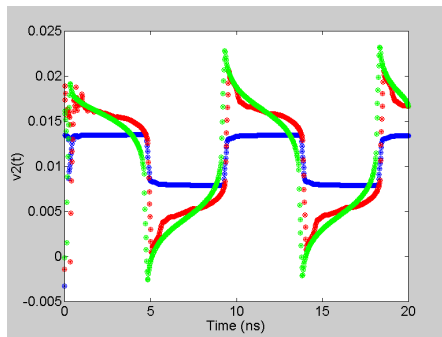one mainly in the trapezoidal-pulse train peak voltages but also in the
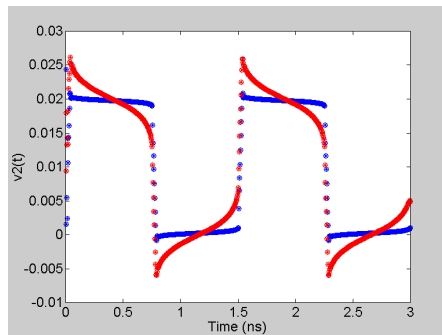
Figure 3. Voltage across the diode terminating the $25\,\Omega$ microstrip
interconnects. Convolution simulation by using the scattering
parameters obtained from the closed-form formulas (blue trace).
Convolution simulation by using the measured scattering parameters
(red trace).
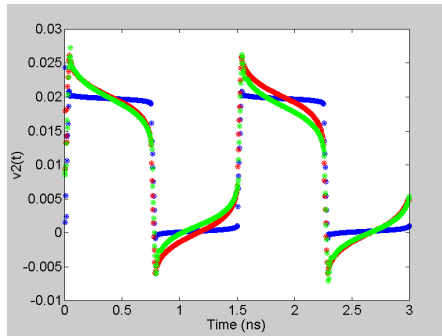
Figure 4. Voltage across the diode terminating the $25\,\Omega$ microstrip interconnects.   Convolution simulation by using the scattering parameters obtained from the closed-form formulas (blue trace). Convolution simulation by using the measured scattering parameters (red trace). Convolution simulation of a three times electrically longer interconnects by using the scattering parameters obtained from the closed-form formulas (green trace).

Figure 5. Voltage across the diode terminating the $50\,\Omega$ microstrip interconnects.   Convolution simulation by using the scattering parameters obtained from the closed-form formulas (blue trace). Convolution simulation by using the measured scattering parameters (red trace). Convolution simulation of one a half time electrically shorter interconnects by using the scattering parameters obtained from the closed-form formulas (green trace).

rise and fall times. The green curve better approximates the red one but an increased bandwidth has been considered in order to increment the electric length $\theta = \beta l$. Thus, in this case, it seems the scattering parameters obtained from the closed-form formulas actually represent

a physically longer microstrip line interconnects. Finally, Fig. 5 shows the convolution simulation responses for the $\varepsilon_r = 3.0$ microstrip line interconnects, once again when the measured scattering parameters (red) and those obtained from the closed-form formulas (blue, and green for a one a half time shorter interconnects) are used. As can be seen from this figure, the red and green traces differ once more from the green one but now the differences are dramatically augmented clearly showing that the S-parameter closed-form formulas fail when wideband simulations are involved.

5. CONCLUSION

The influence of measured scattering parameters on the convolution simulation of nonlinear loaded high-speed microstrip interconnects has been demonstrated mainly when broadband simulations are performed.   The larger the deviation between the analytical and measured scattering parameters, the larger the deviation between the response curves of the convolution simulation.   Thus, in order to do reliable simulations it is advisable to use the measured scattering parameters instead of those of the closed-form formulas until a better set of equations representing well the behaviour of a real microstrip line interconnects be encountered. In addition, the well known theory of microwave reflections was used to strengthen the convolution algorithm by properly settling down the waves on the interconnect line and the voltages and reflection coefficients at source and load.

REFERENCES

1. Tesche, F. M. and T. K. Liu, "Transient response of antennas with non-linear loads," *Electron. Lett.*, Vol. 11, 18–19, Jan. 1975.
2. Liu, T. K. and F. M. Tesche, "Analysis of antennas and scatterers with nonlinear loads," *IEEE Trans. Antennas and Propagat.*, Vol. 24, 131–139, Mar. 1976.

3. Yang, Y. E., J. A. Kong, and Q. Gu, "Time-domain perturbational analysis on nonuniformly coupled transmission lines," *IEEE Trans. Microwave Theory Tech.*, Vol. 33, 1120–1130, Nov. 1985.

4. Gu, Q., Y. E. Yang, and J. A. Kong, "Transient analysis of frequency-dependent transmission line systems terminated with nonlinear loads," *Journal of Electromagnetic Wave and Applications*, Vol. 3, No. 3, 183–197, 1989.

5. Djordjevic, A. R., T. K. Sarkar, and R. F.Harrington, "Analysis of lossy transmission lines with arbitrary nonlinear terminal networks," *IEEE Trans. Microwave Theory Tech.*, Vol. 34, 660–666, Jun. 1986.

6. Djordjevic, A. R., T. K. Sarkar, and R. F. Harrington "Time-domain response of multiconductor transmission lines," *Proceedings of the IEEE*, Vol. 75, 743–764, Jun. 1987.

7. Komuro, T., "Time-domain analysis of lossy transmission lines with arbitrary terminal networks," *IEEE Trans. Circuits Syst.*, Vol. 38, 1160–1164, Oct. 1991.

8. Gu, Q., D. M. Sheen, and S. M. Ali, "Analysis of transients in frequency-dependent interconnections and planar circuits with nonlinear loads," *IEE Proceedings-H*, Vol. 139, 38–44, Feb. 1992.

9. Lin, S. and E. S. Kuh, "Transient simulation of lossy interconnects based on the recursive convolution formulation," *IEEE Trans. Circuits Syst.*, Vol. 39, 879–892, Nov. 1992.

10. Pan, G. W., G. Wang, and B. K. Gilbert, "Analysis of nonlinear termination networks for coupled lossy and dispersive transmission lines," *IEEE Trans. Microwave Theory Tech.*, Vol. 41, 531–535, Mar. 1993.

11. Chu, Q. X., F. Y. Chang, Y. P. Lau, and O. Wing, "Time-domain model synthesis of microstrip," *IEEE Microwave and Guided Wave Lett.*, Vol. 7, 9–11, Jan. 1997.

12. Achar, R. and M. S. Nakhla, "Efficient transient simulation of embedded subnetworks characterized by S-parameters in the presence of nonlinear elements," *IEEE Trans. Microwave Theory Tech.*, Vol. 46, 2356–2363, Dec. 1998.

13. Green, K. and R. Sobolewski, "Extending scattering-parameter approach to characterization of linear time-varying microwave devices," *IEEE Trans. Microwave Theory Tech.*, Vol. 48, 1725–1731, Oct. 2000.

14. Chiang, I. T. and W. C. Chew, "Fast real-time convolution algorithm for transients of nonlinearly-terminated microwave multiport circuits," *Microwave and Optical Tech. Lett.*, Vol. 39,

280–282, Nov. 2003.

15. Li, E. P., E. X. Liu, L. W. Li, and M. S. Leong, "A coupled efficient and systematic full-wave time-domain macromodeling and circuit simulation method for signal integrity analysis of high-speed interconnects," *IEEE Trans. Adv. Pack.*, Vol. 27, 213–223, Nov. 2004.

16. Chiang, I. T. and W. C. Chew, "Fast real-time convolution algorithm for microwave multiport networks with nonlinear terminations," *IEEE Trans. Circuits Syst. II: Analog and Digital Signal Processing*, Vol. 52, 370–375, Jul. 2005.

17. Lee, J. Y., H. H. Lee, and H. K. Jung, "Linear lumped loads in the FDTD method using piecewise linear recursive convolution method," *IEEE Microwave and Wireless Comp. Lett.*, Vol. 16, 158–160, Apr. 2006.

18. Zhong, B., S. L. Dvorak, and J. L. Prince, "Transient simulation of lossy interconnects based on a dispersive hybrid phase-pole macromodel," *IEEE Trans. Adv. Pack.*, Vol. 30, 321–334, May 2007.

19. Tesche, F. M., "On the analysis of a transmission line with nonlinear terminations using the time dependent BLT equation," *IEEE Trans. Electromag. Compat.*, Vol. 49, 427–433, May 2007.

20. Su, D. Y., D. M. Fu, and Z. H. Chen, "Numerical modeling of active devices characterized by measured S-parameters in FDTD," *Progress In Electromagnetics Research*, Vol. 80, 381–392, 2008.

21. Deschrijver, D., T. Dhaene, and D. de Zutter, "Robust parametric macromodeling using multivariate orthonormal vector fitting," *IEEE Trans. Microwave Theory Tech.*, Vol. 56, 1661–1667, Jul. 2008.

22. Lalgudi, S. N., E. Engin, G. Casinovi, and M. Swaminathan, "Accurate transient simulation of interconnects characterized by band-limited data with propagation delay enforcement in a modified nodal analysis framework," *IEEE Trans. Electromag. Compat.*, Vol. 50, 715–729, Aug. 2008.

23. Eudes, T., B. Ravelo, and A. Louis, "Transient response characterization of the high-speed interconnection RLCG-model for the signal integrity analysis," *Progress In Electromagnetics Research*, Vol. 112, 183–197, 2011.

24. Liao, H. and W. Dai, "Scattering parameter transient analysis of interconnect networks with nonlinear terminations using recursive convolution," *Proceedings of the Synthesis and Simulation Meeting and International Interchange*, 295–304, Oct. 1993.

25. Celik, M., L. Pileggi, and A. Obadasioglu, *IC Interconnect Analysis*, Boston, Kluwer, MA, 2002.

26. Chiu, C. N. and I. T. Chiang, "A fast approach for simulating long-time response of high-speed dispersive and lossy interconnects terminated with nonlinear loads," *Progress In Electromagnetics Research*, Vol. 91, 153–171, 2009.

27. Ferranti, F., L. Knockaert, and T. Dhaene, "Parameterized *S*-parameter based macromodeling with guaranteed passivity," *IEEE Microwave and Wireless Comp. Lett.*, Vol. 19, 608–610, Oct. 2009.

28. Ferranti, F., L. Knockaert, and T. Dhaene, "Guaranteed passive parameterized admittance-based macromodeling," *IEEE Trans. Adv. Pack.*, Vol. 33, 623–629, Aug. 2010.

29. Triverio, P., M. Nakhla, and S. Grivet-Talocia, "Passive parametric modeling of interconnects and packaging components from sampled impedance, admittance or scattering data," *3rd Electronic System Integration Technology Conference*, 1–6, Sep. 2010.

30. Triverio, P., M. Nakhla, and S. Grivet-Talocia, "Extraction of parametric circuit models from scattering parameters of passive RF components," *2010 European Microwave Integrated Circuits Conference*, 393–396, Sep. 2010.

31. Ferranti, F., L. Knockaert, T. Dhaene, and G. Antonini, "Passivity-preserving parametric macromodeling for highly dynamic tabulated data based on Lur'e equations," *IEEE Trans. Microwave Theory Tech.*, Vol. 58, 3688–3696, Dec. 2010.

32. Jiménez, A. D., A. S. Santoyo, and F. J. Mendieta, "On the synthesis of some ring junctions for six-port measurement applications," *Microwave Opt. Technol. Lett.*, Vol. 5, 559–563, Oct. 1992.

33. Jiménez, A. D., "Lumped- and distributed-element equivalent circuits for some symmetrical multiport signal-separation structures," *IEEE Trans. Microw. Theory Tech.*, Vol. 45, No. 9, 1537–1544, Sep. 1997.

34. Pozar, D. M., *Microwave Engineering*, 716, John Wiley and Sons, Inc., New York, NY, 1998.

35. Jiménez, A. D., "Estudio de estructuras hexaportales aplicables a analizadores de redes de microondas," Ph.D. Dissertation, Centro de Investigación Científica y de Educación Superior de Ensenada (CICESE), Ensenada, Baja California, México, 1993. Available at: http://biblioteca.cicese.mx/catalogo/tesis/.

36. Montgomery, C. G., R. H. Dicke, and E. M. Purcell, *Principles of Microwave Circuits*, 149, McGraw-Hill, New York, NY, 1948.

37. Collin, R. E., *Foundations for Microwave Engineering*, 170–176, McGraw-Hill, New York, NY, 1966.

38. Jiménez, A. D., *2-D Electromagnetic Simulation of Passive Microstrip Circuits*, 274, CRC Press a Taylor and Francis Company, Boca Raton, Florida, 2009.

39. Jiménez, A. D., "Frequency- and time-domain simulation of microstrip squares by using 2D-FDTD electromagnetic analyses," *International Workshop on Recent Advances in Microwave & Optical Communication Technology Proceedings, in association with 12th Int. Symp. Microw. Opt. Tech.*, SRM University, Chennai, India, Dec. 2009.

40. Jiménez, A. D., "Frequency- and time-domain simulation of microstrip squares by using 2D-FDTD electromagnetic analyses," *Int. Journal Microw. Opt. Tech.*, Vol. 5, 1–6, Jan. 2010.

41. Ambrozkiewicz, M., P. Lorenz, and W. Kraemer, "Equivalent circuits of the transition from coaxial to microstrip transmission line on PCBs," Lecture, Rohde & Schwarz GmbH & Co. KG, Jun. 2008.

42. Peterson, A. F. and G. D. Durgin, *Transient Signals on Transmission Lines: An Introduction to Non-ideal Effects and Signal Integrity Issues in Electrical Systems*, 143, Morgan & Claypool Publishers, San Francisco, California, 2009.

43. Shockley, W., *Electrons and Holes in Semiconductors with Applications to Transistor Electronics*, D. Van Nostrand Company, 1950.

44. Yang, W. Y., W. Cao, T. S. Chung, and J. Morris, *Applied Numerical Methods Using Matlab®*, John Wiley and Sons Inc., 2005.

45. Bandler, J. W., R. M. Biernacki, and S. H. Chen, "Toward direct EM optimization of VLSI interconnects: Validation of coupled transmission line models," *1995 Canadian Conf. Electrical and Computer Engineering*, 377–380, 1995.

46. Sainati, R. A. and T. J. Moravec, "Estimating high speed circuit interconnect performance," *IEEE Trans. Circuits Syst.*, Vol. 36, 533–540, Apr. 1989.